RAA 2019 Vol. **19** No. **9**, 134(8pp) doi: 10.1088/1674–4527/19/9/134

http://www.raa-journal.org *http://iopscience.iop.org/raa*

***R**esearch in*
***A**stronomy and*
***A**strophysics*

A close-in substellar object orbiting the sdOB-type eclipsing-binary system NSVS 14256825

Li-Ying Zhu[1,2,3,4], Sheng-Bang Qian[1,2,3,4], Eduardo Fernández Lajús[5,6], Zhi-Hua Wang[1,2,3,4] and Lin-Jia Li[1,2,3]

[1] Yunnan Observatories, Chinese Academy of Sciences, Kunming 650216, China; *zhuly@ynao.ac.cn*
[2] Key Laboratory of the Structure and Evolution of Celestial Objects, Chinese Academy of Sciences, Kunming 650216, China
[3] Center for Astronomical Mega-Science, Chinese Academy of Sciences, Beijing 100101, China
[4] University of Chinese Academy of Sciences, Beijing 100049, China
[5] Facultad de Ciencias Astronómicas y Geofísicas, Universidad Nacional de La Plata, 1900 La Plata, Buenos Aires, Argentina
[6] Instituto de Astrofisica de La Plata (CCT La Plata C CONICET/UNLP), Paseo del Bosque s/n, La Plata, BA, B1900FWA, Argentina

Received 2019 March 7; accepted 2019 April 24

Abstract NSVS 14256825 is the second discovered sdOB+dM eclipsing-binary system with an orbital period of 2.65 h. This special binary was reported to contain circumbinary planets or brown dwarfs by using the timing method. However, different results were derived by different authors because of the insufficient coverage of eclipse timings. Since 2008, we have monitored this binary for about 10 yr using several telescopes and 84 new times of light minimum were obtained with high precision. It is found that the $O-C$ curve has been increasing recently and it shows a cyclic variation with a period of 8.83 yr and an amplitude of 46.31 seconds. The cyclic change cannot be explained by magnetic activity cycles of the red dwarf component because the required energy is much larger than that radiated by this component in one whole period. This cyclic change detected in NSVS 14256825 could be explained by the light-travel time effect via the presence of a third body. The lowest mass of the third body is determined to be 14.15 $M_{\rm jup}$ which is in the transition range between planets and brown dwarfs. The substellar object is orbiting around this evolved binary at an orbital separation of around 3 AU with an eccentricity of 0.12. These results indicate that NSVS 14256825 is the first sdOB-type eclipsing binary consisting of a hierarchical substellar object. The detection of a close-in substellar companion to NSVS 14256825 will provide some insights on the formation and evolution of sdOB-type binaries and their companions.

Key words: binaries: close — binaries: eclipsing — stars: evolution — stars: individual (NSVS 14256825)

1 INTRODUCTION

HW Virginis (HW Vir) binaries are a group of detached eclipsing-binary systems that consist of a very hot subdwarf B or OB type primary and a fully convective M-type secondary with periods usually shorter than 4 h. They are believed to be formed through a common envelope ejection (Heber 2009, 2016). The hot sdB-type components in this group of binaries are on the extreme horizontal branch (EHB) of the Hertzsprung-Russell diagram, burning helium in their cores and having very thin hydrogen envelopes. They have very high temperature and similar size compared to their M-type companions, which cause the eclipse profiles of this type of binary to be very sharp and deep. Benefiting from this characteristic, the light arrival time of the binary can be measured to a high precision (e.g., Kilkenny 2011, 2014). Therefore, small wobbles caused by the orbits of other substellar companions can be discovered. To date, this timing method is the most successful one to be applied to the detection of substellar objects orbiting evolved stars, such as giant planets orbiting around the eclipsing white dwarf bina-

ries DE CVn (Han et al. 2018) and RR Cae (Qian et al. 2012a), around eclipsing polars DP Leo (Qian et al. 2010a; Beuermann et al. 2011) and HU Aqr (Qian et al. 2011; Goździewski et al. 2015), around eclipsing dwarf nova V2051 Oph (Qian et al. 2015), etc. Up till now, the reported HW Vir-type binaries have been rare, numbering not more than 20. Some of them have been found to be the hosts of substellar objects using the timing method, i.e., HW Vir (Qian et al. 2008; Lee et al. 2009; Beuermann et al. 2012a), HS 0705+6700 (Qian et al. 2008, 2013; Beuermann et al. 2012b), NY Vir (Qian et al. 2012b), HS 2231+2441 (Almeida et al. 2014, 2017), OGLE-GD-ECL-11388 (Hong et al. 2017), 2M 1938+4603 (Baran et al. 2015), etc.

With an orbital period of 2.65 h, NSVS 14256825 (= V1828 Aql = 2MASS J20200045+0437564 = UCAC2 33483055 = USNO-B1.0 0946-0525128) (hereafter NSVS 1425) is an HW Vir-like eclipsing binary possibly containing hierarchical substellar companions. Its light variability was found in the public data release from the Northern Sky Variability Survey (NSVS, Woźniak et al. 2004). Wils et al. (2007) carried out multi-band CCD observations and obtained the first group times of light minimum for NSVS 1425 with a high precision (with uncertainties of less than 0.0002 d). Almeida et al. (2012) analyzed their $UBVR_cI_cJH$ light curves and radial velocity curve simultaneously using the Wilson-Devinney code, and provided reliable fundamental parameters of NSVS 1425 as $M_1 = 0.419 \pm 0.070\,M_\odot$, $M_2 = 0.109 \pm 0.023\,M_\odot$, $R_1 = 0.188 \pm 0.010\,R_\odot$, $R_2 = 0.162 \pm 0.008\,R_\odot$ and $i = 82.5° \pm 0.3°$. They pointed out that NSVS 1425 is an sdOB+dM eclipsing binary. Qian et al. (2010b) and Zhu et al. (2011) found a hint about cyclic period change in this system. Kilkenny & Koen (2012) suggested that the period of NSVS 1425 is rapidly increasing at a rate of about 12×10^{-12} d orbit^{-1}. Beuermann et al. (2012b) reported that there may be a giant planet with a mass of roughly 12 $M_{\rm Jup}$ in NSVS 1425. Almeida et al. (2013) revisited its $O-C$ curve and explained the changes in the $O-C$ diagram by the presence of two circumbinary bodies with masses of 2.9 $M_{\rm Jup}$ and 8.1 $M_{\rm Jup}$. Wittenmyer et al. (2013) presented a dynamical analysis of the orbital stability of the model suggested by Almeida et al. (2013). They found that a two-planet model of NSVS 1425 is unstable on timescales of less than a thousand years. Later, Hinse et al. (2014) concluded that insufficient coverage of the timing data prevents reliable constraints of the associated parameters. Recently, Nasiroglu et al. (2017) published their new times of light minimum, which extended the time span to November 2016. Their best-fitting model ruled out the two-planet model and reported a cyclic change that was explained as the presence of a brown dwarf. However, their data still do not cover a full cycle.

It has been shown that the chemical compositions and evolutionary statuses of sdOB- and sdB-binary stars are quite different (e.g., Heber 2016). On the T-$\log g$ diagram given by Almeida et al. (2012), the position of the primary component of NSVS 1425 is close to that of the primary of the first sdOB-type binary AA Dor, but is far away from those of other sdB-type binaries. The investigations by Kilkenny (2011, 2014) demonstrated that the $O-C$ curve of AA Dor is constant indicating that no substellar objects are orbiting around it. Therefore, whether there are any substellar objects orbiting NSVS 1425 is a very interesting question. In this paper, we present our 84 newly determined high precision timings for NSVS 1425 obtained from observations between Dec. 2008 and Dec. 2018, which effectively extend the baseline of the timing data and cover more than a full cycle of the cyclic variation in the $O-C$ diagram. Combined with high precision timings collected from the literature, we perform a new orbital period investigation of this HW Vir-type binary.

2 OBSERVATIONS AND DATA REDUCTION

We have been monitoring a group of HW Vir-like eclipsing binaries since 2006. For NSVS 1425, we began to observe it in December 2008 with several small telescopes in China and Argentina, i.e., the 2.4-m and 70-cm telescopes at the Lijiang Station of Yunnan Observatories, Chinese Academy of Sciences (YNO), 1.0-m and 60-cm telescopes at the Kunming Station of YNO (YNO 2.4-m, YNO 70-cm, YNO 1-m and YNO 60-cm), the 2.16-m and 85-cm telescopes at the Xinglong Station of National Astronomical Observatories, Chinese Academy of Sciences (NAOC; NAOC 2.16-m and NAOC 85-cm respectively), and the 2.15-m Jorge Sahade telescope at Complejo Astronómico El Leoncito (CASLEO; CASLEO 2.15-m), San Juan, Argentina. These seven telescopes are all equipped with CCD cameras and the standard Johnson−Cousin−Bessel BVR_cI_c filters. Using these telescopes, we obtained observations covering ten years from December 2008 to December 2018. All image reductions were done by applying the IRAF package. Seventy-two primary eclipsing profiles and 12 secondary eclipsing profiles were obtained. They all display symmetric light variations. To derive the times of light minimum, we modeled these eclipsing profiles using the amplitude of a Gaussian peak function

$$G(t) = m_0 + Ae^{-\frac{(t-t_c)^2}{2w}}. \quad (1)$$

In this function, m_0 is the offset; A is the amplitude; t_c is the timing and w is the width with $2w = \mathrm{FWHM}/\sqrt{\ln(4)}$.

Table 1 New Times of Light Minimum for NSVS 1425

BJD	Error (d)	E	$O-C$ (d)	Telescope	BJD	Error (d)	E	$O-C$ (d)	Telescope
2454818.90501	0.00005	4935	–0.000258	NAOC 85cm	2456047.36959	0.00001	16065	0.000235	YNO 60cm
2454933.36268	0.00005	5972	–0.000562	YNO 60cm	2456069.33405	0.00004	16264	0.000243	YNO 60cm
2454936.34294	0.00008	5999	–0.000403	YNO 60cm	2456069.38926	0.00008	16264.5	0.000266	YNO 60cm
2454961.39796	0.00003	6226	–0.000311	YNO 1.0m	2456164.14541	0.00003	17123	0.000218	NAOC 85cm
2454963.38463	0.00007	6244	–0.000376	YNO 60cm	2456219.11183	0.00002	17621	0.000322	YNO 1.0m
2454968.24111	0.00003	6288	–0.000358	YNO 60cm	2456234.01231	0.00003	17756	0.000294	YNO 60cm
2454969.23445	0.00008	6297	–0.000385	YNO 60cm	2456248.96791	0.00008	17891.5	0.000199	YNO 60cm
2454969.28957	0.00013	6297.5	–0.000452	YNO 60cm	2456249.02323	0.00004	17892	0.000332	YNO 60cm
2454972.38013	0.00002	6325.5	–0.000367	YNO 2.4m	2456373.41486	0.00013	19019	0.000308	YNO 60cm
2454986.23200	0.00004	6451	–0.000446	YNO 2.4m	2456440.30158	0.00007	19625	0.000306	YNO 1.0m
2454994.28935	0.00006	6524	–0.000413	YNO 60cm	2456456.30576	0.00003	19770	0.000236	YNO 1.0m
2455000.24974	0.00005	6578	–0.000226	YNO 60cm	2456514.14177	0.00001	20294	0.000223	NAOC 85cm
2455031.26470	0.00010	6859	–0.000397	YNO 1.0m	2456533.12611	0.00003	20466	0.000192	YNO 1.0m
2455104.11174	0.00004	7519	–0.000284	YNO 2.4m	2456557.07731	0.00003	20683	0.000206	YNO 1.0m
2455118.01888	0.00001	7645	–0.000289	YNO 2.4m	2456758.39958	0.00001	22507	0.000060	YNO 2.4m
2455118.07402	0.00003	7645.5	–0.000336	YNO 2.4m	2456823.18914	0.00003	23094	0.000004	NAOC 85cm
2455118.12921	0.00002	7646	–0.000328	YNO 2.4m	2456908.17717	0.00006	23864	–0.000048	YNO 1.0m
2455146.05390	0.00001	7899	–0.000294	YNO 2.4m	2456960.05296	0.00001	24334	–0.000100	YNO 2.4m
2455153.00750	0.00004	7962	–0.000264	NAOC 85cm	2456962.03971	0.00009	24352	–0.000084	YNO 2.4m
2455165.03824	0.00002	8071	–0.000305	YNO 2.4m	2456966.01314	0.00003	24388	–0.000123	YNO 1.0m
2455296.38336	0.00011	9261	–0.000400	YNO 60cm	2456972.96670	0.00001	24451	–0.000133	NAOC 85cm
2455333.35878	0.00004	9596	–0.000314	YNO 2.4m	2456973.96007	0.00001	24460	–0.000131	NAOC 85cm
2455334.35217	0.00001	9605	–0.000291	YNO 2.4m	2457187.25783	0.00008	26392.5	–0.000384	NAOC 85cm
2455380.15742	0.00002	10020	–0.000305	YNO 1.0m	2457278.04048	0.00003	27215	–0.000458	NAOC 85cm
2455437.11053	0.00013	10536	–0.000256	YNO 60cm	2457933.82780	0.00004	33156.5	–0.001046	CASLEO 2.15m
2455438.10395	0.00007	10545	–0.000203	YNO 60cm	2457933.88289	0.00001	33157	–0.001143	CASLEO 2.15m
2455444.17447	0.00002	10600	–0.000260	NAOC 2.16m	2457991.60849	0.00001	33680	–0.001216	CASLEO 2.15m
2455445.05746	0.00002	10608	–0.000263	YNO 1.0m	2457991.66373	0.00003	33680.5	–0.001163	CASLEO 2.15m
2455450.02436	0.00005	10653	–0.000199	NAOC 85cm	2458008.16467	0.00002	33830	–0.001156	YNO 2.4m
2455453.11482	0.00002	10681	–0.000215	NAOC 85cm	2458011.14475	0.00002	33857	–0.001178	YNO 2.4m
2455499.03051	0.00002	11097	–0.000163	NAOC 85cm	2458019.53317	0.00001	33933	–0.001183	CASLEO 2.15m
2455688.32227	0.00004	12812	–0.000034	NAOC 85cm	2458019.58832	0.00004	33933.5	–0.001230	CASLEO 2.15m
2455692.29572	0.00003	12848	–0.000053	NAOC 85cm	2458019.64351	0.00001	33934	–0.001227	CASLEO 2.15m
2455700.35324	0.00012	12921	0.000156	YNO 60cm	2458287.79745	0.00005	36363.5	–0.001233	CASLEO 2.15m
2455721.32418	0.00011	13111	0.000011	YNO 60cm	2458287.85272	0.00002	36364	–0.001150	CASLEO 2.15m
2455737.32837	0.00001	13256	–0.000047	YNO 2.4m	2458288.73570	0.00002	36372	–0.001163	CASLEO 2.15m
2455783.35435	0.00004	13673	–0.000089	YNO 2.4m	2458366.05278	0.00006	37072.5	–0.001164	YNO 60cm
2455784.12698	0.00008	13680	–0.000078	NAOC 85cm	2458366.10801	0.00004	37073	–0.001121	YNO 60cm
2455798.14458	0.00002	13807	0.000008	YNO 2.4m	2458451.97914	0.00002	37851	–0.001070	YNO 70cm
2455872.09538	0.00002	14477	0.000141	YNO 2.4m	2458460.97453	0.00008	37932.5	–0.001173	YNO 70cm
2455879.04895	0.00001	14540	0.000141	YNO 2.4m	2458461.02974	0.00005	37933	–0.001150	YNO 70cm
2455883.02224	0.00006	14576	–0.000038	YNO 60cm	2458462.02315	0.00002	37942	–0.001108	YNO 70cm

Table 2 Orbital Parameters of NSVS 1425 and its Circumbinary Substellar Object

Parameters	Values
Correction to the initial epoch, T_0 (d)	$2.87(\pm0.10)\times10^{-4}$
Revised period, P (d)	$0.1103741030(\pm0.0000000005)$
LTT amplitude, K (d)	$0.000536(\pm0.000005)$
Eccentricity, e	$0.12(\pm0.02)$
Orbital period, P_3 (yr)	$8.83(\pm0.06)$
Longitude of the periastron passage, ω (deg)	$133.3(\pm10.3)$
Periastron passage, T (HJD)	$2456816.0(\pm93.7)$
Projected semi-major axis, $a_{12}\sin i^{'}$ (AU)	$0.0928(\pm0.0009)$
Mass function, $f(m)$ $(M_{\odot})$	$9.63(\pm0.32)\times10^{-6}$
Mass of the third body, M_3 $(M_{\rm Jup}, i'=90^{\circ})$	$14.15(\pm0.16)$
Orbital separation, d_3 (AU, $i'=90^{\circ}$)	$3.12(\pm0.07)$

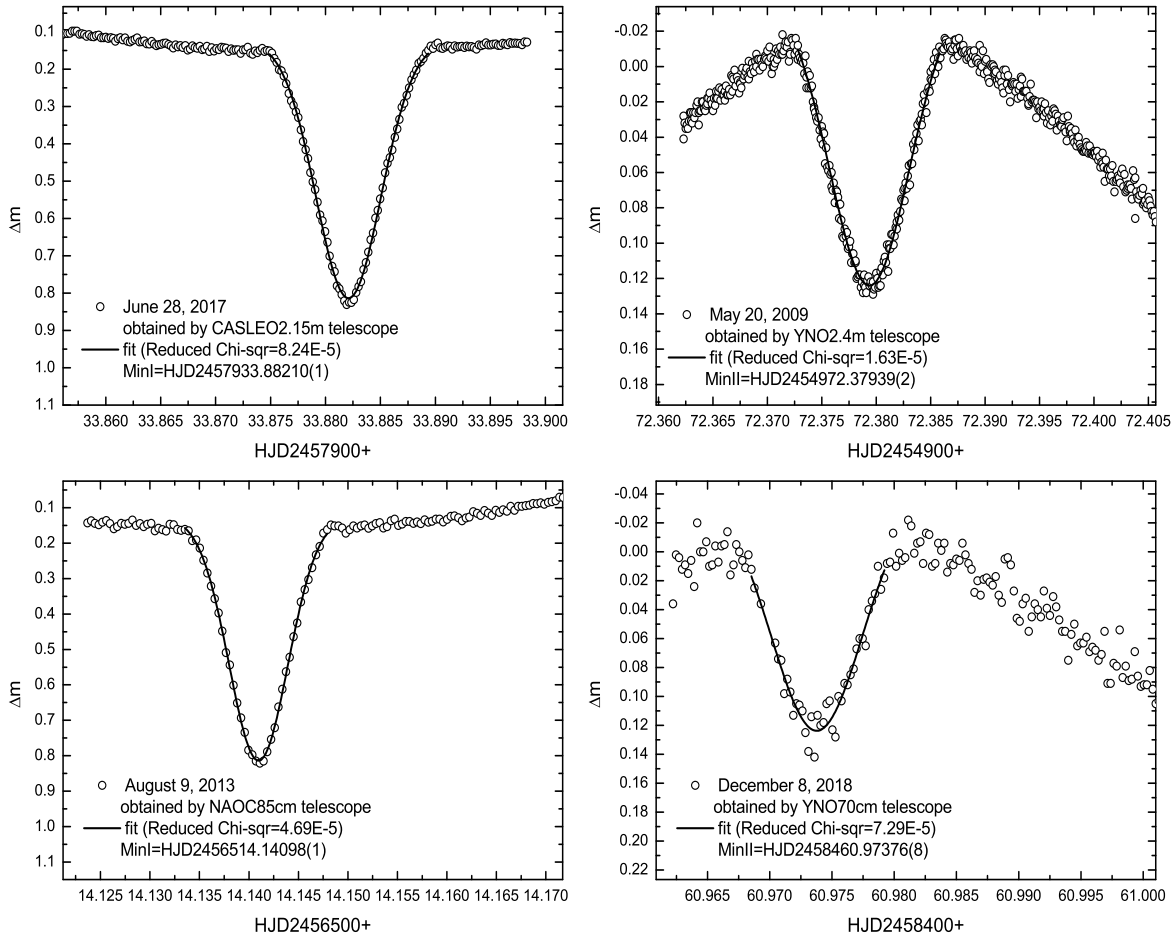

Fig. 1 Some eclipsing profiles of NSVS 1425. *Open circles* are the observations and *solid lines* are the fit curves. The light curves displayed in the upper panels were obtained by 2-m class telescopes, while those in the lower panels were acquired by 1-m class telescopes. The left panels depict the primary eclipsing profiles and the right panels plot the secondary ones.

Figure 1 depicts some examples of the observed eclipsing light curves (open circles) and the corresponding fits (solid lines). All the derived times of light minimum are listed in Table 1.

3 ORBITAL PERIOD INVESTIGATION

Based on the times of light minimum, several authors have studied the $O-C$ diagram of NSVS 1425. Among them, Nasiroglu et al. (2017) collected the most comprehensive timings up to the end of 2016. By adding our new eclipse times, we calculated the cycle number E and the $O-C$ values according to the following ephemeris from Beuermann et al. (2012b)

$$\begin{aligned}\mathrm{Min.}I(\mathrm{BJD}) =& 2454274.208923(4) \\ &+ 0.1103741324(3)^{\mathrm{d}} \times E\,.\end{aligned} \quad (2)$$

The newly constructed $O-C$ curve extends the coverage baseline for another two years, which is plotted in Figure 2. Our $O-C$ values calculated from new timings are signified with green dots, while others are displayed with blue dots. From this figure, one can see that another minimum in the $O-C$ curve has been caught, enabling analysis based on one full cycle of the periodical variation. As the light-travel time effect (LTT) signals caused by the low mass or/and long period objects are small, low precision timings may lead to this signal being submerged in scattered points, such as in the case of EG Cep (Zhu et al. 2009). Therefore, we just use the timings with errors smaller than 0.0002 to reconstruct the $O-C$ curve and display it in the upper panel of Figure 3. The cyclic variation is obvious in this figure. To describe the $O-C$ curve, the following equation was used

$$O-C = \Delta T_0 + \Delta P_0 \times E + \tau, \quad (3)$$

where ΔT_0 and ΔP_0 are, respectively, the revised epoch and period with respect to the ephemeris values in

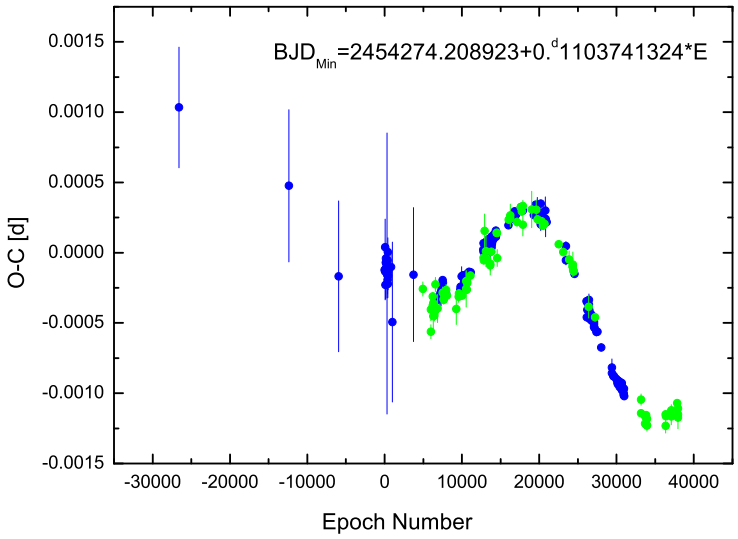

Fig. 2 The $O-C$ diagram of the HW Vir-type binary NSVS 1425 is constructed based on all available timings. *Green dots* are derived from our new data.

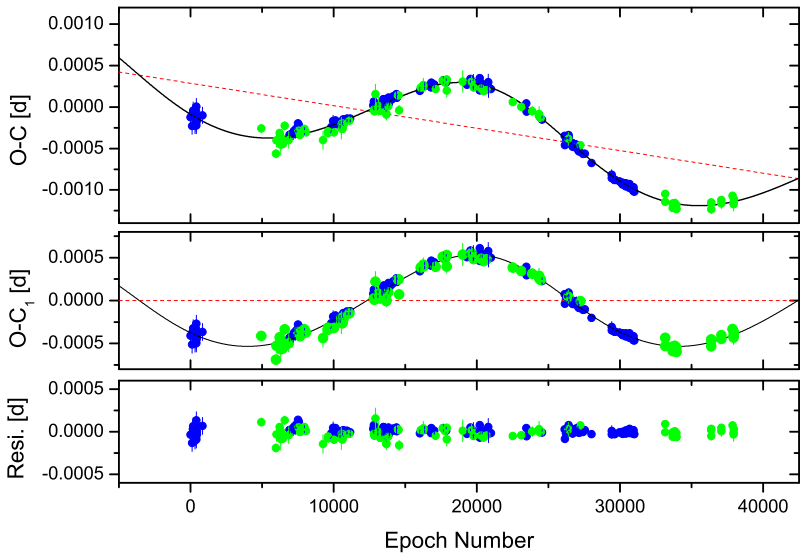

Fig. 3 The $O-C$ diagrams of the HW Vir-type binary NSVS 1425 constructed from the high precision timings. *Green dots* refer to the data newly obtained by us, and *blue dots* to data collected from the literature. The *solid line* in the top panel represents a combination of a revised linear ephemeris (the *dashed red line*) and a periodic variation (also signified as the *solid line* in the middle panel where the $(O-C)_1$ values were calculated with respect to the revised linear ephemeris). The residuals are displayed in the bottom panel where no variations can be traced there.

Equation (2). τ is described by Irwin (1952) as the cyclic change term due to the LTT caused by a third body

$$\tau = K[(1-e^2)\frac{\sin(\nu+\omega)}{1+e\cos\nu} + e\sin\omega] = K[\sqrt{1-e^2}\sin E^*\cos\omega + \cos E^*\sin\omega]\,. \quad (4)$$

In this equation, e is the eccentricity, ν is the true anomaly, ω is the longitude of the periastron passage in the plane of the orbit and E^* is the eccentric anomaly. $K = a\sin i^{'}/c$ is the projected semi-major axis given in days, where a is the semi-major axis of the elliptic orbit. By means of the Levenberg-Marquardt method, the results of the nonlinear fit for the $O-C$ diagram are obtained. The solid line in the top panel of Figure 3 represents a combination of a revised linear ephemeris and a periodic variation. All derived parameters are listed in Table 2. The revised period is $0.1103741030(5)$ d.

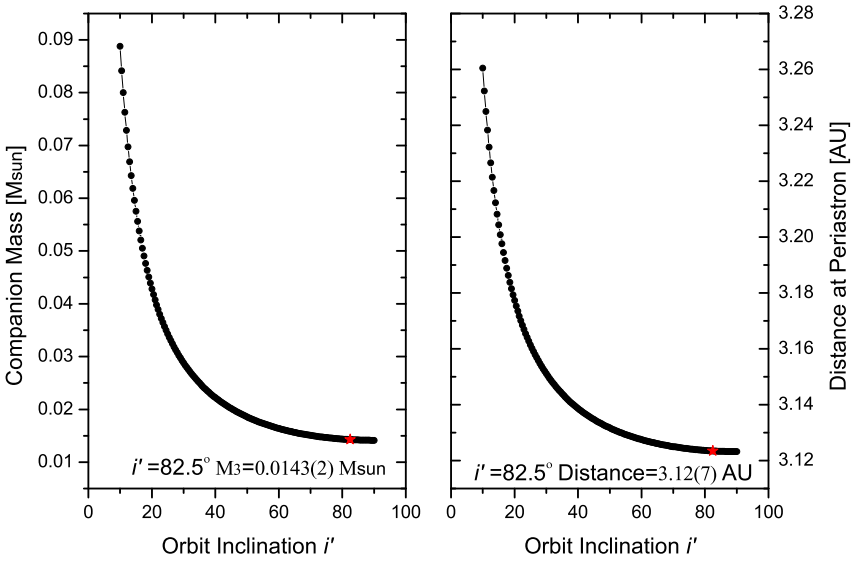

Fig. 4 Relations between the mass M_3 and distance at periastron d_3 of the third body and its orbital inclination $i^{'}$ in the NSVS 1425 system. The *red stars* represent the value when its orbital plane is coplanar with the orbital plane of the inner binary (*Color version is online*).

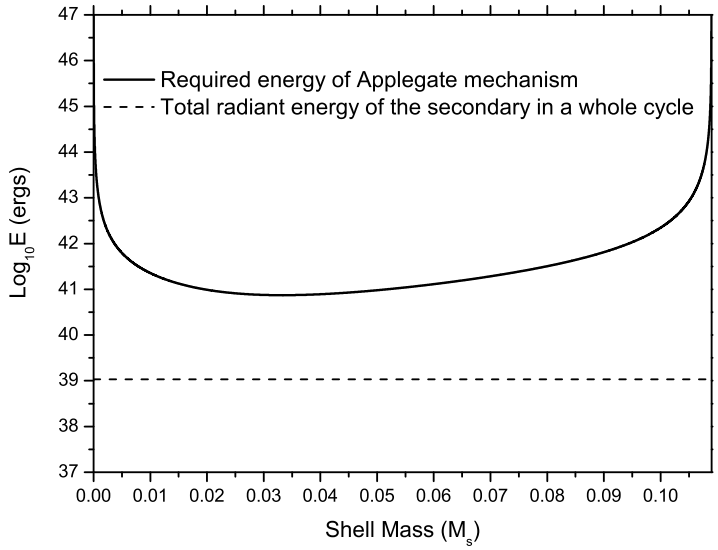

Fig. 5 Energy required to produce cyclic oscillation in the $O-C$ diagrams using Applegate's mechanism (*solid line*). M_s is the assumed shell mass of the cool component. The *dashed line* represents the total energy that radiates from the fully convective red dwarf secondary in one whole period ~ 8.83 yr.

Our final result indicates that the $O-C$ curve shows a cyclic change with a period of $8.83(6)$ yr and an amplitude of $0.000536(5)$ d that can be seen more clearly in the middle panel of Figure 3. The residuals are depicted in the bottom panel and its standard deviation is 0.00005. The results demonstrate that the third body in NSVS 1425 has a minimal mass of 14.15 $M_{\rm Jup}$, which orbits the central HW Vir-type binary in an eccentric orbit with $e \sim 0.12(2)$.

4 DISCUSSION AND CONCLUSIONS

NSVS 1425 is the second HW Vir-type eclipsing binary consisting of a very hot subdwarf OB-type primary and a fully convective M-type secondary. Its sdOB primary lies in the EHB of the Hertzsprung-Russell diagram, having a very high temperature of about 40 000 K (Almeida et al. 2013) and small size with radius 0.19 $R_{\odot}$, while its M dwarf secondary has very low temperature and small size

compared to the sdOB primary. Thanks to these characteristics, the eclipsing profiles produced by them are very sharp and deep, which means that the light arrival time of the central object can be measured to a high precision and therefore its small wobbles caused by the orbiting of substellar companions can be discovered. Due to the high surface gravities and compact structures of sdB, sdOB or white dwarfs, both the radial velocity and transit methods (which have been extensively employed to search for planets around solar-type main-sequence stars) have a low efficiency in detecting substellar companions (exoplanets or brown dwarfs) of those post-red giant branch stars. Instead, this timing method, based on the LTT, is the most successful one to be applied to finding substellar objects orbiting such evolved stars, and is similar to the radio approach used to discover planets around pulsars (Wolszczan & Frail 1992; Backer et al. 1993).

We have monitored NSVS 1425 for ten years and obtained 84 new high precision times of light minimum, which effectively extended the baseline of the data and covered another minimum in the $O-C$ curve, facilitating a full cycle constructed by the high precision data. Based on these data, we reanalyzed the $O-C$ diagram and found a cyclic oscillation with an amplitude of 0.00053 d (or 45.8 s) and a period of 8.83 yr, which can be explained by the wobble of the binary's barycenter via the existence of a third body. Our updated parameters confirmed that there is a hierarchical substellar object orbiting around the central sdOB+dM type eclipsing binary with an orbital eccentricity of 0.12. The relationship between the mass (M_3) and distance at periastron (d_3) varying along with the inclination of the tertiary component ($i^{'}$) is shown in Figure 4. The distance at periastron (d_3) of this tertiary component ranges from 3.26 AU to 3.12 AU as its inclination ($i^{'}$) varies from 10 deg to 90 deg, implying that this tertiary component is a close-in object. When the orbital plane of this third body is coplanar with the orbital plane of the inner binary, its mass (M_3) should be $14.3\,M_{\rm Jup}$, which lies in the boundary zone between planets and brown dwarfs.

As suggested by many authors, the cyclic period oscillations of close binaries comprised of cool star components can also be explained by magnetic activity cycles (Applegate 1992). For NSVS 1425, the secondary component is a fully convective red dwarf star with a mass of $0.109\,M_{\odot}$ and an effective temperature of 2550 K (Almeida et al. 2012). In order to check this possibility, we computed the energies required to cause this cyclic period change using the same method proposed by Brinkworth et al. (2006) and plotted its relationship with the assumed shell mass of the secondary in Figure 5 (solid line). The dashed line in Figure 5 represents the total energy that radiates from the fully convective red dwarf secondary in one whole period (8.83 yr). One can see that the required energies are much larger than the total energy radiated from the secondary star in one whole period. Therefore, the cyclic change cannot be explained by magnetic activity cycles of the secondary component in NSVS 1425.

Some sdB eclipsing binaries have been reported with substellar objects orbiting around them, but not sdOB eclipsing binaries. NSVS 1425 is the first one. For single sdB- and sdO-stars, their chemical compositions and evolutionary statuses are quite different. sdB stars are mostly helium poor, while sdO stars manifest a variety of helium abundances (e.g., Heber 2016). Moreover, most sdB stars were found in binary systems, while the binary frequency of sdO stars is very low. These properties may indicate that their formations are different. As for the two sdOB eclipsing binary stars, AA Dor and NSVS 1425, although they are located in the same region on the T-$\log g$ diagram (e.g., Almeida et al. 2012), the properties of their tertiary companions are quite different. A close-in substellar object is orbiting NSVS 1425, but no known substellar objects are orbiting around AA Dor (e.g., Kilkenny 2011, 2014). If the circumbinary substellar object in NSVS 1425 is formed from the remaining common-envelope material (second generation planets), why are there no substellar objects orbiting around AA Dor? Maybe AA Dor and NSVS 1425 have different formation channels. The detection of the close-in substellar object orbiting around NSVS 1425 will provide us with more information on the formation and evolution of sdOB-type binaries and their companions.

Acknowledgements This work is partly supported by the National Natural Science Foundation of China (No. 11573063), the Key Science Foundation of Yunnan Province (No. 2017FA001), CAS "Light of West China" Program and CAS Interdisciplinary Innovation Team. New CCD photometric observations of NSVS 14256825 were obtained with the 2.16-m and 85-cm telescopes at Xinglong Station of NAOC, the 2.4-m, 1.0-m, 60-cm and 70-cm telescopes at the YNOs, and the 2.15-m telescope at Complejo Astronómico El Leoncito (CASLEO), San Juan, Argentina.

References

Almeida, L. A., Jablonski, F., Tello, J., & Rodrigues, C. V. 2012, MNRAS, 423, 478

Almeida, L. A., Jablonski, F., & Rodrigues, C. V. 2013, ApJ, 766, 11

Almeida, L. A., Damineli, A., Jablonski, F., Rodrigues, C. V., & Cieslinski, D. 2014, in Revista Mexicana de Astronomia y Astrofisica, 44, 35

Almeida, L. A., Damineli, A., Rodrigues, C. V., Pereira, M. G., & Jablonski, F. 2017, MNRAS, 472, 3093
Applegate, J. H. 1992, ApJ, 385, 621
Backer, D. C., Foster, R. S., & Sallmen, S. 1993, Nature, 365, 817
Baran, A. S., Zola, S., Blokesz, A., Østensen, R. H., & Silvotti, R. 2015, A&A, 577, A146
Beuermann, K., Buhlmann, J., Diese, J., et al. 2011, A&A, 526, A53
Beuermann, K., Dreizler, S., Hessman, F. V., & Deller, J. 2012a, A&A, 543, A138
Beuermann, K., Breitenstein, P., Debski, B., et al. 2012b, A&A, 540, A8
Brinkworth, C. S., Marsh, T. R., Dhillon, V. S., & Knigge, C. 2006, MNRAS, 365, 287
Goździewski, K., Słowikowska, A., Dimitrov, D., et al. 2015, MNRAS, 448, 1118
Han, Z.-T., Qian, S.-B., Zhu, L.-Y., et al. 2018, ApJ, 868, 53
Heber, U. 2009, ARA&A, 47, 211
Heber, U. 2016, PASP, 128, 082001
Hinse, T. C., Lee, J. W., Goździewski, K., Horner, J., & Wittenmyer, R. A. 2014, MNRAS, 438, 307
Hong, K., Lee, J. W., Lee, D.-J., et al. 2017, PASP, 129, 014202
Irwin, J. B. 1952, ApJ, 116, 211
Kilkenny, D. 2011, MNRAS, 412, 487
Kilkenny, D. 2014, MNRAS, 445, 4247
Kilkenny, D., & Koen, C. 2012, MNRAS, 421, 3238
Lee, J. W., Kim, S.-L., Kim, C.-H., et al. 2009, AJ, 137, 3181
Nasiroglu, I., Goździewski, K., Słowikowska, A., et al. 2017, AJ, 153, 137
Qian, S.-B., Dai, Z.-B., Zhu, L.-Y., et al. 2008, ApJ, 689, L49
Qian, S.-B., Liao, W.-P., Zhu, L.-Y., & Dai, Z.-B. 2010a, ApJ, 708, L66
Qian, S.-B., Zhu, L.-Y., Liu, L., et al. 2010b, Ap&SS, 329, 113
Qian, S.-B., Liu, L., Liao, W.-P., et al. 2011, MNRAS, 414, L16
Qian, S.-B., Liu, L., Zhu, L.-Y., et al. 2012a, MNRAS, 422, L24
Qian, S.-B., Zhu, L.-Y., Dai, Z.-B., et al. 2012b, ApJ, 745, L23
Qian, S.-B., Shi, G., Zola, S., et al. 2013, MNRAS, 436, 1408
Qian, S. B., Han, Z. T., Fernández Lajús, E., et al. 2015, ApJS, 221, 17
Wils, P., di Scala, G., & Otero, S. A. 2007, Information Bulletin on Variable Stars, 5800
Wittenmyer, Robert A., Horner, J., & Marchall, J. P. 2013, MNRAS, 431, 2150
Wolszczan, A., & Frail, D. A. 1992, Nature, 355, 145
Woźniak, P. R., Vestrand, W. T., Akerlof, C. W., et al. 2004, AJ, 127, 2436
Zhu, L. Y., Qian, S. B., Liao, W. P., et al. 2009, PASJ, 61, 529
Zhu, L., Qian, S., Liu, L., et al. 2011, in Astronomical Society of the Pacific Conference Series, 451, 9th Pacific Rim Conference on Stellar Astrophysics, eds. S. Qain, K. Leung, L. Zhu, & S. Kwok, 155